Supporting Information

Park et al. 10.1073/pnas.0904004106

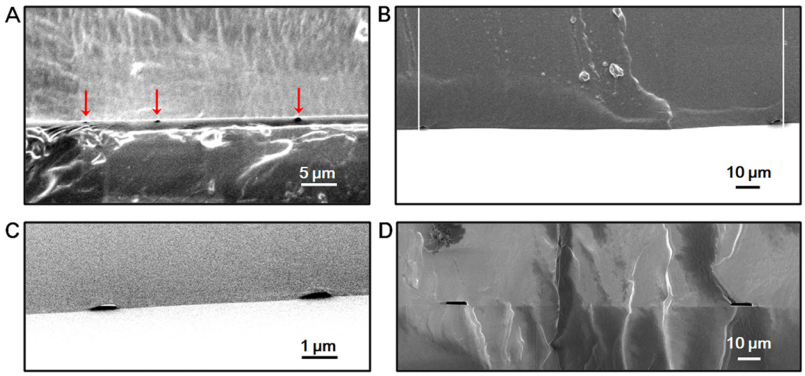

Fig. S1. Various SEM images of nanochannels with different configurations. (*A*) Nanochannels 10 and 20 μm apart from each other at the PDMS-PDMS interface. (*B*) Nanochannels (100 μm apart) formed at a PDMS-cover glass interface. (*C*) Nanochannels (10 μm apart) formed by roof collapse at a PDMS-cover glass interface. The lateral and vertical dimensions of the nanochannels shown here are smaller than 1 μm. (*D*) Microchannels with 10 $\times$ 1.4 μm dimensions that are resistant to roof collapse.

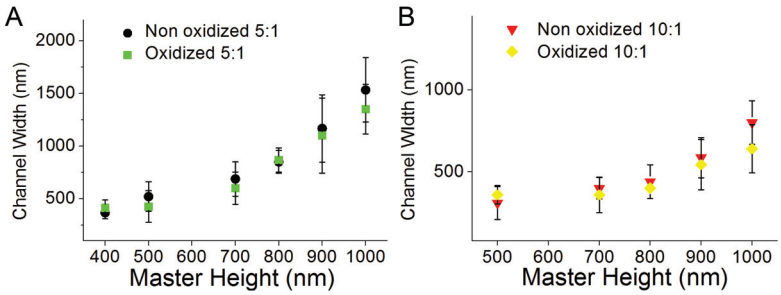

Fig. S2. Plots of channel width against master height for both 10:1 PDMS and 5:1 PDMS. (*A*) Relationship between the PDMS master height and nanochannel width for 5:1 elastomer base/curing agent mixture. There is no significant channel width difference in the oxidized PDMS and non-oxidized PDMS. (*B*) Relationship between the PDMS master height and nanochannel width for10:1 elastomer base/curing agent mixture. Again, no significant difference in nanochannel width was found in comparing both non-oxidized and oxidized PDMS.

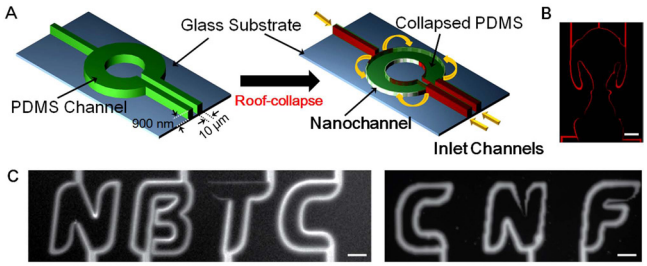

Fig. S3. Optical images showing various PDMS micro-/nanochannel designs. (*A*) Schematic illustration of the ''O'' letter formation using this method. We note that because the nanochannel layout matches that of its master, the nanochannels can be formed into very complex patterns without much restraint (so long as the master holds a looped curve). (*B*) Micro- and nanofluidic representations of Snoopy (cartoon character) image (Scale bar, 50 μm). (*C*) CNF and NBTC Logo without oxdization process (Scale bars, 50 μm).

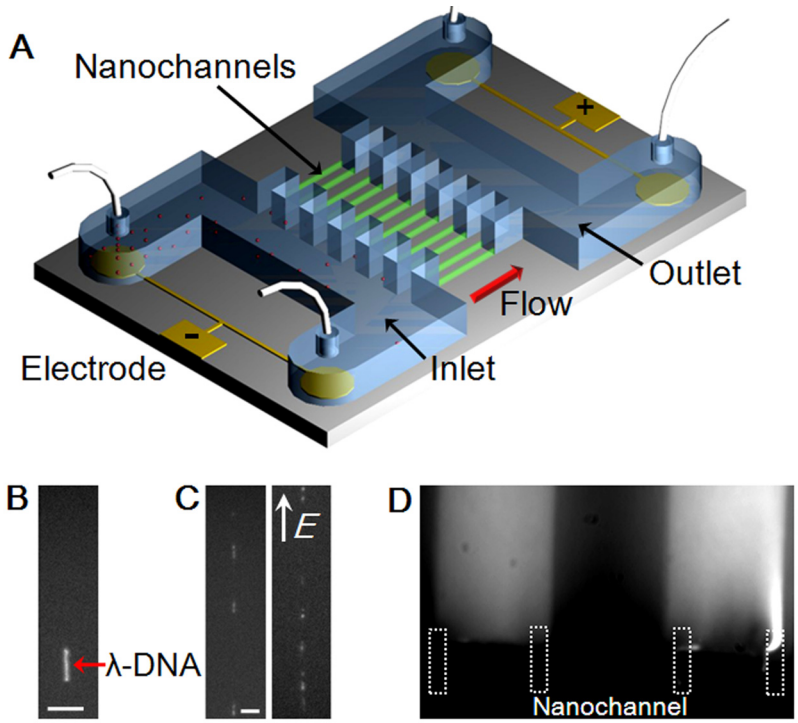

Fig. S4. Micro-/nanofluidic device for DNA elongation and nanoparticle concentration. (*A*) Schematic representation of the nanofluidic device. (*B*) Fluorescent image of the stationary λ-DNA elongated along the nanochannel (no external electric field applied; Scale bar, 5 μm). (*C*) Fluorescent images of λ-DNAs elongated along the nanochannels. Two different lengths of elongated DNA are shown for the different nanochannel sizes (Scale bar, 2 μm). (*D*) Concentration of 45-nm polystyrene nanoparticles at the interface between the microchannel and nanochannel. The same micro-/nanofluidic interface used in Fig. 5*C* is shown. The ''Bottle Neck'' effect of the micro-/nano-interfaces amasses the nanoparticles despite their being smaller than the nanochannels. The operating electric field is 40 V cm^{-1}.

Table S1. Success rate of nanochannel formation under various conditions including: master width, master height, with and without plasma oxidation, and different elastomer base: curing agent ratios

		Non-Oxidized PDMS			Oxidized PDMS		
		Elastomer base:Curing agent base ratios					
Master width, μm	Master height, nm	5:1	10:1	15:1	5:1	10:1	15:1
10	300	25.6 ± 5.3	43.2 ± 7.2	A	91.3 ± 8.2	92.6 ± 7.8	A
	400	19.4 ± 3.1	39.2 ± 4.2	87.8 ± 3.2	31.7 ± 6.2	65.8 ± 4.7	A
	500	15.7 ± 3.2	32.4 ± 3.8	77.4 ± 4.3	53.3 ± 7.7	61.2 ± 5.4	83.6 ± 3.2
	700	7.3 ± 2.3	31 ± 4.5	18.4 ± 4.9	43.7 ± 8.7	52.2 ± 7.6	45.3 ± 6.3
	800	2.5 ± 1.1	7.3 ± 2.3	8.2 ± 2.1	6.7 ± 2.6	9.8 ± 3.4	9.3 ± 3.7
	900	N	2.7 ± 1.2	7.5 ± 2.5	4.2 ± 1.9	6.5 ± 2.8	8.6 ± 2.6
	1,000	N	2.5 ± 0.7	5.2 ± 3.1	3.6 ± 0.8	5.5 ± 2.1	7.8 ± 3.8
20	300	72.3 ± 5.2	94.5 ± 5.7	A	95.7 ± 5.2	A	A
	400	39.7 ± 4.6	48.9 ± 6.4	A	81.4 ± 3.9	94.2 ± 6.9	A
	500	33.4 ± 5.1	40.3 ± 6.7	94.3 ± 6.4	62.5 ± 4.7	71.4 ± 4.6	A
	700	15.3 ± 3.3	28.7 ± 5.6	85.3 ± 7.5	58.9 ± 3.7	65.6 ± 6.5	95.3 ± 5.4
	800	7.4 ± 2.5	9.5 ± 3.9	35.7 ± 4.8	10.8 ± 2.3	12.7 ± 4.5	55.3 ± 7.4
	900	N	3.7 ± 1.7	21.2 ± 4.5	8.6 ± 2.3	9.5 ± 3.2	45.5 ± 5.3
	1000	N	2.5 ± 0.5	8.7 ± 3.3	7.1 ± 1.8	8.2 ± 2.6	9.5 ± 2.9
50	300	95.4 ± 5.7	A	A	A	A	A
	400	94.7 ± 6.2	A	A	A	A	A
	500	63.7 ± 4.2	94.5 ± 6.7	A	94.1 ± 6.5	94.9 ± 6.3	A
	700	23.4 ± 5.9	44.8 ± 5.7	A	71.4 ± 5.3	82.2 ± 4.5	A
	800	7.7 ± 2.1	19.3 ± 3.7	95 ± 5.3	28.7 ± 6.3	45.7 ± 4.6	A
	900	5.1 ± 1.5	11.7 ± 2.3	83.1 ± 6.7	23.4 ± 4.1	25.7 ± 5.3	96.5 ± 5.7
	1,000	N	9.3 ± 2.3	69.5 ± 5.4	21.5 ± 4.5	15.3 ± 3.2	85.3 ± 6.2
100	300	94.5 ± 7.4	A	A	A	A	A
	400	94.1 ± 6.3	A	A	A	A	A
	500	93.7 ± 7.4	A	A	94.5 ± 6.7	A	A
	700	75.4 ± 5.9	95.5 ± 5.3	A	92.4 ± 5.4	95.1 ± 6.6	A
	800	39.2 ± 4.8	64.3 ± 4.7	A	92.1 ± 4.6	94.6 ± 5.4	A
	900	26.3 ± 5.7	40.2 ± 4.2	96.7	70.3 ± 6.3	83.4 ± 4.3	A
	1,000	7.5 ± 2.4	27.3 ± 6.7	94.2	45.7 ± 4.7	58.4 ± 5.9	A

A and N represent ″annihilation″ and ″NO-collapse″, respectively.